LIGHTCURVE ANALYSIS FOR FOURTEEN NEAR-EARTH ASTEROIDS OBSERVED 2003 - 2022

Peter Birtwhistle
Great Shefford Observatory
Phlox Cottage, Wantage Road
Great Shefford, Berkshire, RG17 7DA
United Kingdom
peter@birtwhistle.org.uk

(Received: 2023 January 4)

Lightcurves and amplitudes for 14 small near-Earth asteroids observed from Great Shefford Observatory during close approaches between 2003 and 2022 are reported. All are superfast rotators with periods shorter than the 2.2 h spin barrier, 8 with periods shorter than 3 minutes and include 6 with reliably detected or suspected tumbling motion.

Photometric observations of near-Earth asteroids during close approaches to Earth between 2003 and November 2022 were made at Great Shefford Observatory using a 0.30-m Schmidt-Cassegrain and Apogee AP47p CCD camera (pre-2005 September) and a 0.40-m Schmidt-Cassegrain and Apogee Alta U47+ CCD camera from 2005 September onwards. All observations were made unfiltered and with the telescopes operating with a focal reducer at f/6. The 1K×1K, 13-micron CCDs were binned 2×2 resulting in an image scale of 3.0 arcsec/pixel (0.30-m telescope) and 2.16 arcsec/pixel (0.40-m telescope). All the images were calibrated with dark and flat frames and *Astrometrica* (Raab, 2018) was used to measure photometry using APASS Johnson V band data from the UCAC4 catalogue (Zacharias et al., 2013) unless otherwise stated. *MPO Canopus* (Warner, 2022), incorporating the Fourier algorithm developed by Harris (Harris et al., 1989) was used for lightcurve analysis.

No previously reported results for any of the objects reported here have been found in the Asteroid Lightcurve Database (LCDB) (Warner et al., 2009), from searches via the Astrophysics Data System (ADS, 2022) or from wider searches unless otherwise noted. All size estimates are calculated using H values from the Small-Body Database Lookup (JPL 2022a), using an assumed albedo for NEAs of 0.2 (LCDB readme.pdf file) and are therefore uncertain and offered for relative comparison only.

2003 EM1. This Aten was discovered at 16th mag from Črni Vrh on 2003 Mar 5.92 UTC and made an approach to 4 Lunar Distances (LD) 27 hours later (Tichy et al., 2003). It was observed for an hour starting at 2003 Mar 6.09 UTC when the apparent speed was 54 arcsec/min and 95 exposures of 4 s duration and 2 of 10 s were obtained. The resulting analysis indicates a 1.0 magnitude amplitude lightcurve with a rotation period of 0.03097 ± 0.00002 h at phase angle 29.1°. A previously reported result with $P = 0.030968 \pm 0.000003$ h and amplitude 0.6 (Behrend, 2003web) obtained from measurements made over the period 2003 Mar 7.8 - 2003 Mar 8.8 UTC, when the phase angle ranged from 18 - 23° is in good agreement with this result.

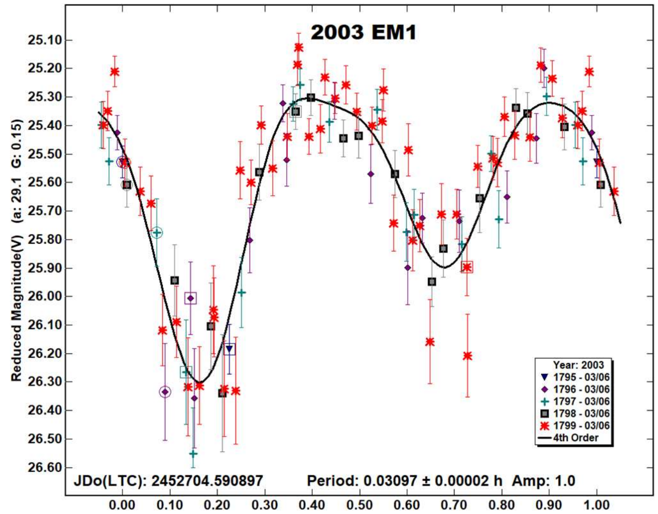

2008 EZ7. A ~12 m diameter Apollo discovered by the Siding Spring Survey using the 0.5-m Uppsala Schmidt on 2008 Mar 7.49 UTC (Gilmore et al., 2008), it passed Earth at a geocentric distance of 0.42 LD on 2008 Mar 9.06 UTC. It was observed over a period of 2.4 h starting less than an hour after closest approach when its topocentric distance increased from 0.41 to 0.48 LD and apparent speed reduced from 620 to 470 arcsec/min. A range of exposures of 0.2, 0.4, 0.6 and 1 second were taken, but the photometric reduction uses 189 measurements from just the 0.6 and 1 s exposures, the shorter exposures being unsuitable for measurement due to both low SNr and, especially for the 0.2 s images, uneven illumination of the field as the CCD shutter opened and closed. The period spectrum shows a number of short period solutions, with the best fit producing a bimodal lightcurve of period 0.016514 h = 59 s.

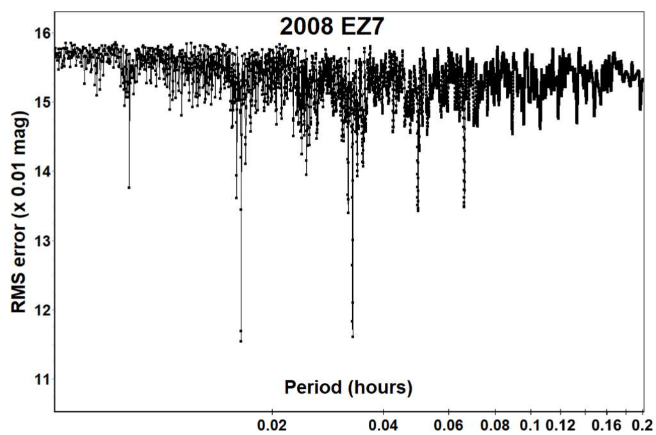

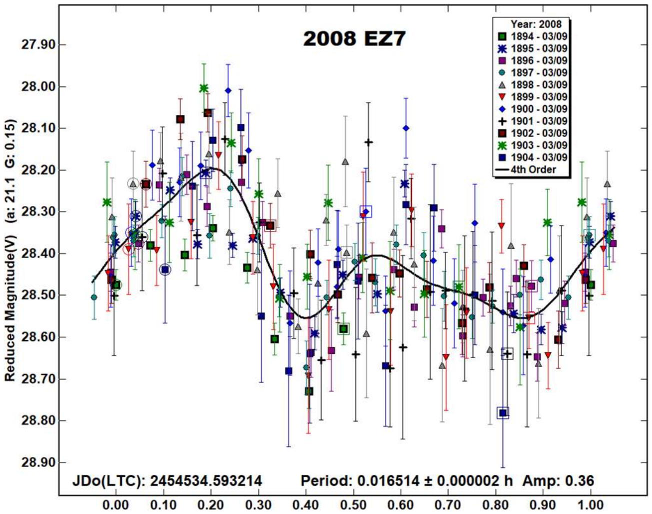

2011 EY11. This small Apollo (H=28.5, dia. ~6 m) was discovered by the Catalina Sky Survey on 2011 Mar 3.56 UTC (Hill et al., 2011), already less than 5 LD from Earth and 43 hours ahead of a close approach to 0.34 LD. It was observed extensively on its approach from Great Shefford over the 4-hour period 2011 Mar 6.91 -7.08 UTC when its distance decreased from 0.7 - 0.4 LD. Apparent sky motion increased from 280 to 924 arcsec/min and exposures of 1 s, decreasing to 0.5 s were used throughout to reduce image trailing. Phase angle reached a minimum for the apparition at 15.5°, 10 minutes before observations began and only reached 39.2° by the end of the session. Large amplitude variations were visible in consecutive images and an initial reduction of the lightcurve (labelled as PAR) indicated a very fast rotation period of 65 s and amplitude of 0.74.

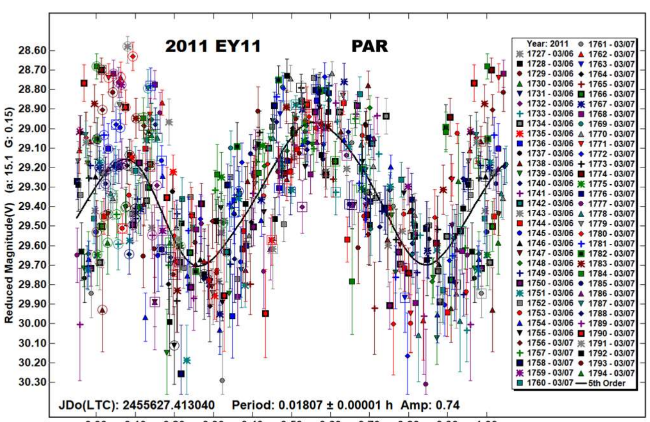

However, more scatter is apparent in the first maxima than the two minima in the bimodal curve, indicating the possibility of tumbling or non-principal axis (NPA) rotation being present. A linearly scaled period spectrum covering periods from 24 - 240 s shows multiple potential solutions and on inspection these appear to consist of two sets of equally spaced values, here labelled P1 (spaced by 32.5 s) and P2 (spaced by 45.2 s).The Dual Period Analysis function in *MPO Canopus* was then used to attempt a NPA solution and even though not designed for this type of analysis it did manage to locate a period of 65 s and, after iterative subtractions, also a secondary period of 90 s, the lightcurves here are labelled P1 and P2 respectively. As the two periods are well resolved it is expected that the rotation may be characterised using the coding described in Pravec et al. (2005) with a PAR code of -3, i.e., *NPA rotation reliably detected with the two periods resolved*. (Petr Pravec, personal communication).

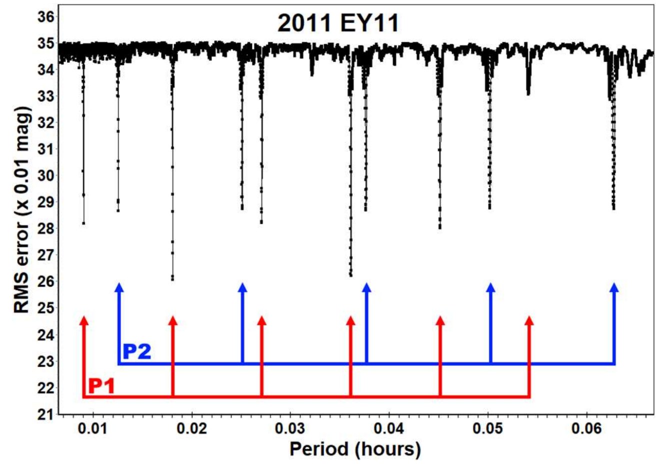

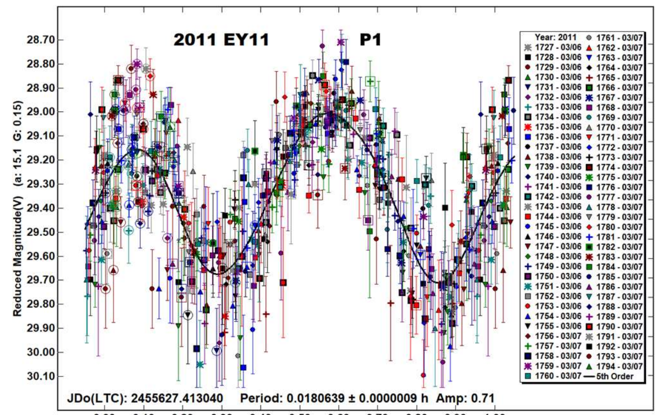

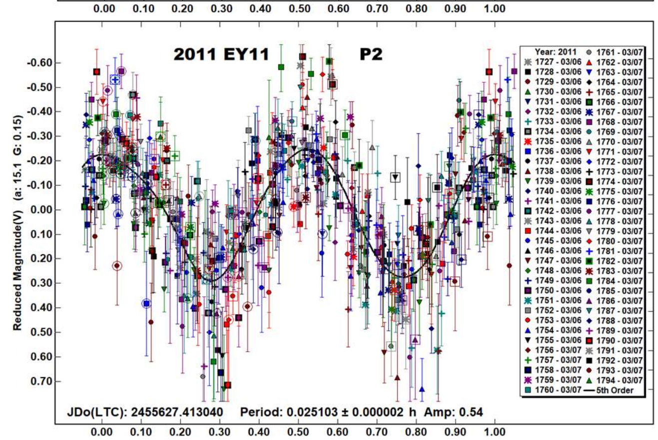

2011 MD. Following discovery by LINEAR on 2011 June 22.26 UTC this asteroid made a very close approach to Earth on 2011 June 27.71 UTC, to 12,300 km of the Earth's surface (Blythe et al., 2011). It has been relatively well studied for such a small body due in part to its potential as a candidate for a spacecraft mission (JPL, 2022b), its diameter being estimated to be in the range 4 - 10 m (Mommert et al., 2014). It was observed for 1.6 h starting on 2011 June 27.01 UTC and photometry was measured using *Astrometrica* in the Gaia G band against reference stars from the Gaia DR2 catalogue. Analysis in *MPO Canopus* resulted in the best fit lightcurve having a period of 0.196361 ± 0.000012 h and amplitude 0.74 ± 0.11 with the RMS of scatter around the Fourier curve being 0.078 magnitudes. There are a number of previously published results listed in the LCDB, all obtained between 2011 June 25 - 28, with Ryan and Ryan (2012) and Skiff et al. (2022) reporting results in close agreement with this determination and Apitzsch (2011web), Franco (2011web) and Vaduvescu et al. (2017)

reporting double that period, near 0.39 h. Trying to fit the longer period to the data points in this paper results in the RMS increasing by 29% to 0.101 magnitudes and a Split Halves plot in *MPO Canopus* shows the two halves matching to within 0.04 magnitudes, supporting the adoption of the shorter period in this determination.

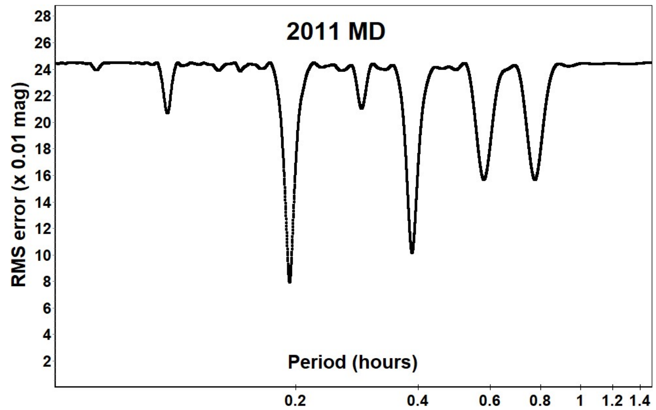

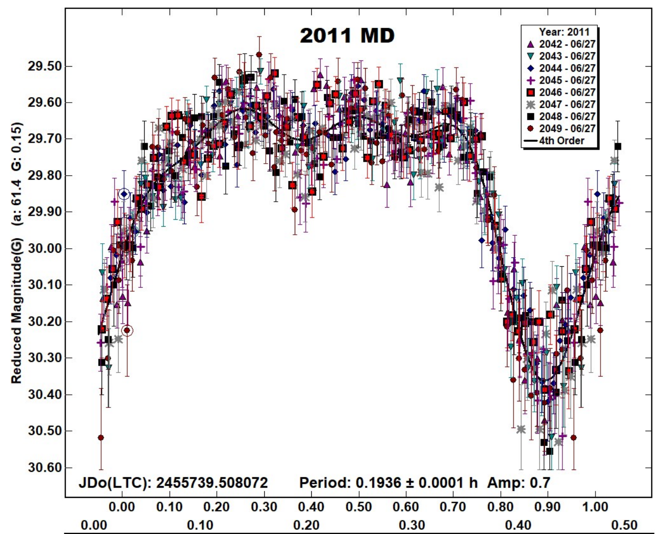

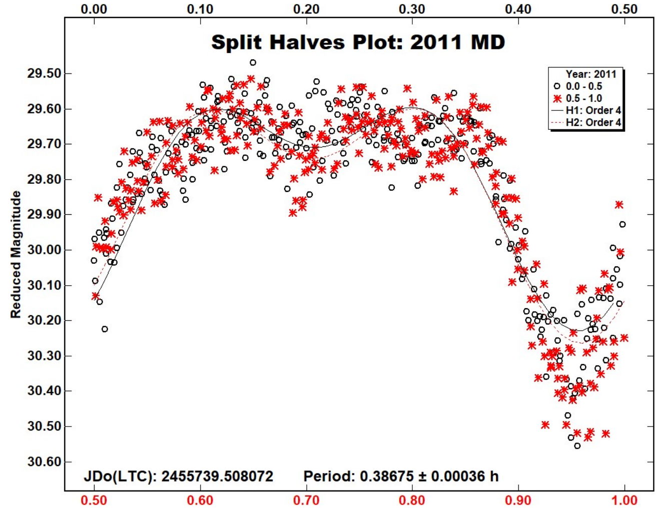

2012 FP35. This small Apollo asteroid was discovered by the Catalina Sky Survey 48 hours before it passed Earth at 0.4 LD (Buzzi et al., 2012). During its final approach it was followed from 2012 Mar 25.841 - 25.948 UTC when the phase angle reduced from 9.6° to a minimum of 9.5°, then increased to 10.6°. After a gap of 2.76 h, it was then followed again from 2012 Mar. 26.063 - 26.088 UTC during which time the phase angle increased from 19.2° to 22.8°. Over the two sets of observations the telescope had to be repositioned a total of 33 times. Apparent speed increased from 100 to 450 arcsec/minute as the distance to the NEO decreased from 1.3 to 0.6 LD, with exposures being reduced from 2 to 1 and finally to 0.5 seconds due to the increasing speed.

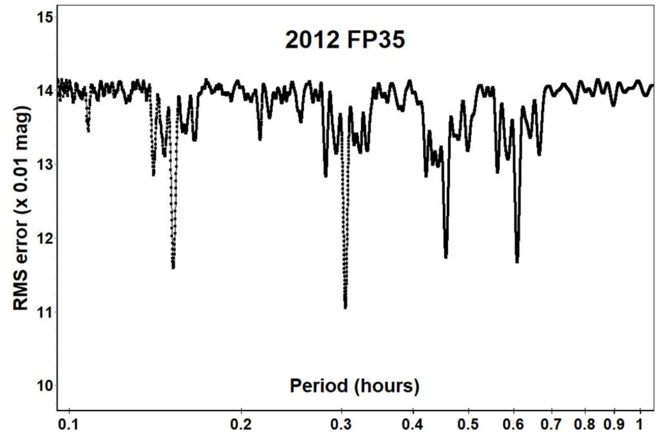

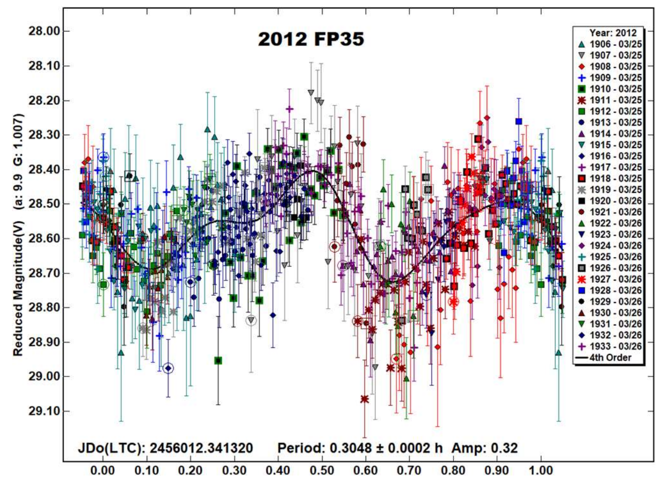

The lightcurve analysis indicated that a phase slope parameter (G) of 0.15 was inadequate to model the observed changes as the phase increased from 9.6° to 22.8°, with less fading observed than was predicted. Therefore, to independently determine the absolute magnitude Hv and the phase slope parameter G, the apparent magnitudes for each of the 33 individual sessions were averaged, corrected for unit distance and entered into the *MPO Canopus* H/G Calculator.

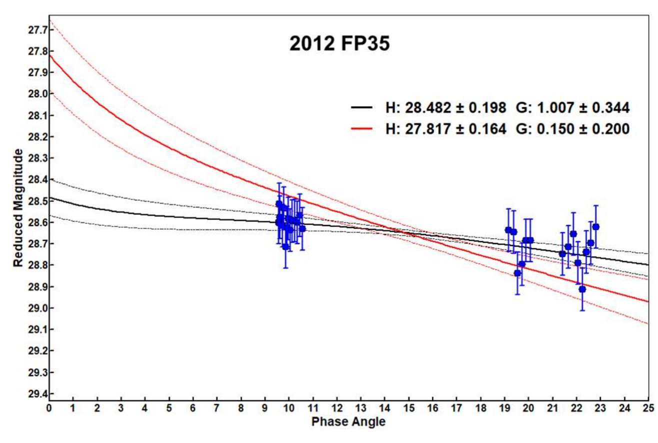

A plot of the resulting best fit solution gives Hv = 28.482 ± 0.198 and G = 1.007 ± 0.344 and is used to produce the phased lightcurve plot. The Minor Planet Center uses a value of Hv = 27.9 using an assumed value of G = 0.15 (MPC, 2022). Forcing the H/G Calculator to use a value of G = 0.15 results in a value of Hv = 27.82 ± 0.16 and G = 0.15 ± 0.20, in good agreement with the MPC, but providing a poorer lightcurve fit.

2016 GP221. Another Catalina Sky Survey discovery, found on 2016 Apr 14.34 UTC (Knoefel et al., 2016) and with H = 25.9 its estimated diameter is ~20 m. It passed Earth at 1.5 LD four days later and was observed for a total of 28 minutes over a period of 1.3 h starting at 2016 Apr 18.03 UTC. Apparent speed rose from 280 to 320 arcsec/minute and exposures were limited to 1 second throughout. The best fit to the 124 measurements gave a rather noisy bimodal lightcurve with a 54 second period and 1 magnitude amplitude.

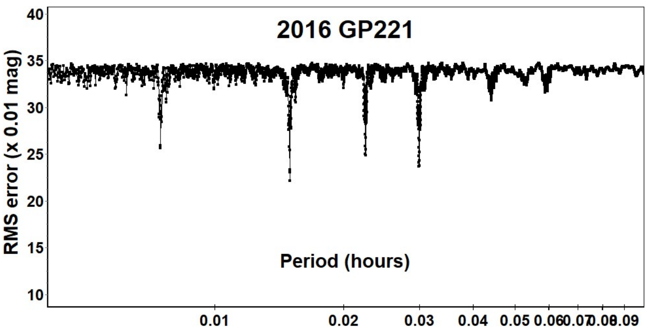

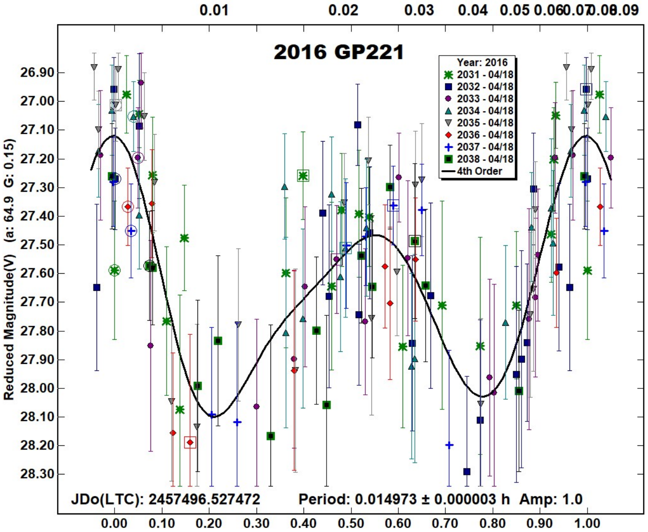

2017 TE5. This was discovered by the Catalina Sky Survey 3 days before an approach to 1.3 LD and with H = 26.0 has an estimated diameter of ~19 m (Janda et al., 2017). It was observed for 4 minutes starting at 2017 Oct 16.900 UTC and then again 4.65 h later for 16 minutes, the telescope needed to be repositioned 3 times for the later imaging due to the high apparent speed of 180 arcsec/min. and exposures were limited to 2 seconds throughout. Analysis of the first set of observations with *MPO Canopus* produced a lightcurve with an amplitude of 0.52 mags and period of 0.02250 ± 0.00015 h, indicating that 2.8 revolutions had been covered in the 4 minutes of observations. The second set of observations also produced a similar lightcurve of amplitude 0.65 mags and a period of 0.022102 ± 0.000013 h, with 12 rotations being covered. Using the latter as the better-defined period, the likely error in number of rotations ΔN between the two sets of observations was estimated using eq. (3) in Kwiatkowski et al. (2010):

$$\Delta N \approx \Delta t\, \Delta P / P^2$$

where Δt is the time interval separating the two lightcurves, P is the period from one of the individual solutions and ΔP is the maximum period uncertainty, with Δt, ΔP and P expressed in the same units. This gives ΔN ≈ 0.1, indicating that the two sets of observations can be matched to a tenth of a rotation and so the two data sets can be unambiguously combined, this producing the phased lightcurve with period of 0.0221192 ± 0.0000006 h. It is noted that there is a zero-point issue between the first and second set of measurements, with the first session requiring an adjustment of -0.18 mags to minimize scatter in the overall lightcurve and this has been applied in the phased curve given here. An equivalent fit can also be obtained using the unusually large value of G = 1.286 which then implies H_v = 27.34, but with observations taken at just two short ranges of phase angles (at 9.3° and 15.4-16.1°) there is not enough data to verify whether that relationship is valid.

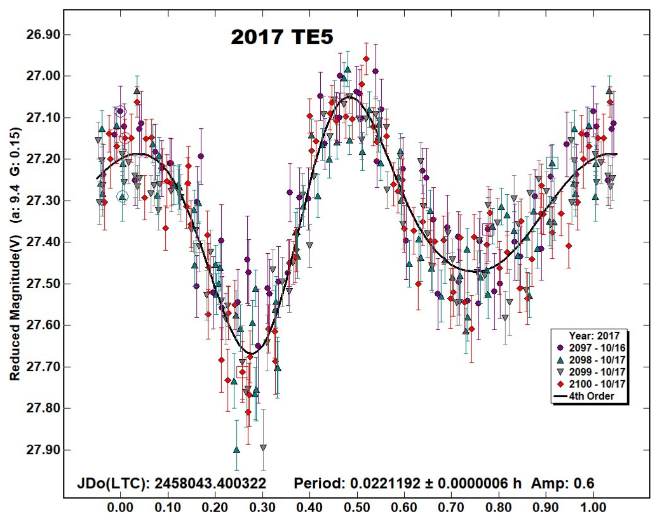

2018 SM1. The Minor Planet Center classifies this object as an Amor because its perihelion distance, q = 1.004 AU is > 1, but using a slightly different definition, the JPL SBDB lists 2018 SM1 as an Apollo, q being less than the Earth's aphelion distance of 1.017 AU and therefore the orbit is considered to be Earth-crossing. With H = 22.9 it has an estimated diameter of ~78m and following discovery by ATLAS on 2018 Sep 18 (Lehmann et al., 2018) it spent the next 9 days between apparent mag +16 and +17. It was followed over three consecutive nights, 2018 Sep 26.9, 27.9 and 29.0 UTC when the ephemeris magnitude was forecast to drop from mag +16.4 to +16.7. Observations were collected on the three nights for 2.7, 2.1 and 1.3 h respectively and raw diagrams of the three nights show variability, with maxima and minima on the last two nights occurring approximately every 25 minutes. However, the first night shows less regular variation and, with the amplitude also decreasing throughout the second night, it is possible that the object may be tumbling. However, the *MPO Canopus* Dual Period Search function could not resolve a consistent solution across all three nights. A phased solution from the second and third nights only is given, indicating an apparent bimodal lightcurve of period 1.598 h. It is suspected that 2018 SM1 is tumbling but not conclusively, so would be rated as PAR = -1 (*NPA rotation possible, some deviations from the single periodicity are seen but not at a conclusive level*) on the scale of Pravec et al. (2005).

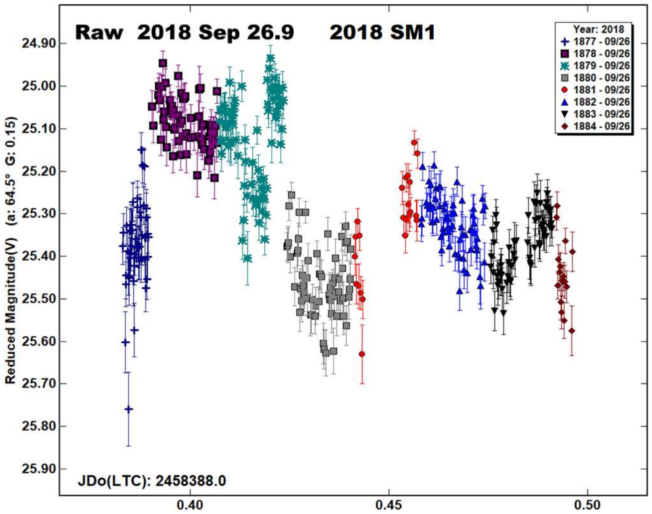

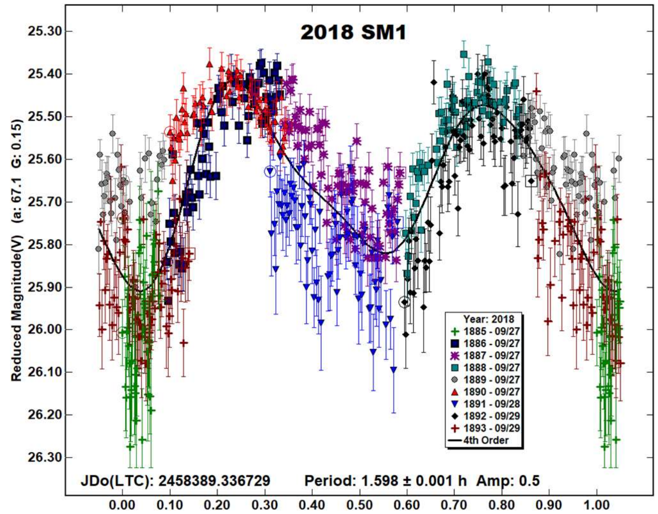

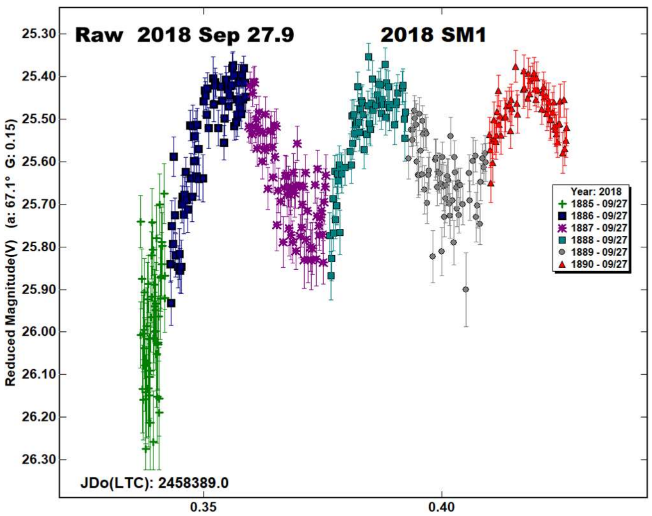

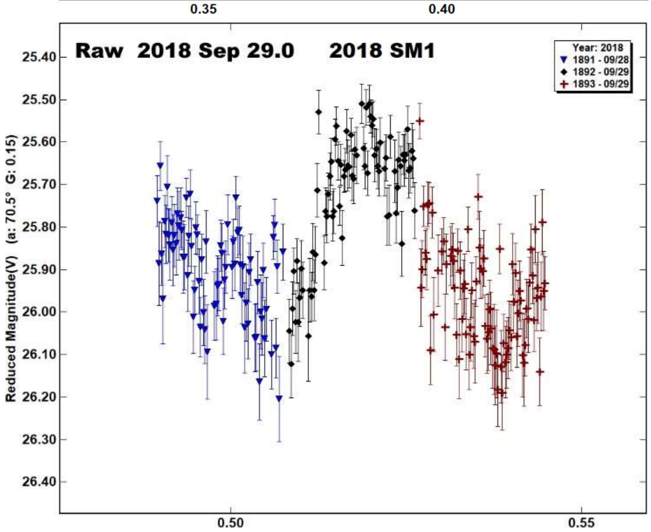

2018 ST1. This Apollo was discovered by the ZTF team at Palomar on 2018 Sept 22.24 UTC and only observed for 65 hours which covered either side of a close approach to 4.3 LD from Earth on 2018 Sept 24.28 UTC (Bacci et al., 2018). It was followed for 4.4 h at Great Shefford starting at 2018 Sept 23.87 UTC. Apparent motion was 85 arcsec/min and 2081 images were obtained, exposures being limited to 2 and 5 s throughout. Visual inspection of the raw images showed large brightness variations with maxima occurring approximately every 15 minutes. However, it was too faint to see on individual images during some minima and therefore, for further analysis the images were stacked using *Astrometrica*. Assuming a bimodal lightcurve, the rotation period was expected to be ~30 minutes, this was used to estimate the optimum effective exposure length Δt for a rotation period P to maximize SNR with minimal lightcurve smoothing, from $\Delta t = 0.185$ P (Pravec et al., 2000). In this case $\Delta t = 0.185 \times 30$ min = 5.6 min was taken as an upper limit on effective exposure length. In case the real period was actually somewhat shorter, the images were then arranged in groups for stacking so that the maximum time from start of first image to end of last image in any one stack was at most 2.5 minutes but generally shorter. Five measurements with a SNR of 3 or less were excluded from the analysis, leaving a total of 155 points from the stacked images for the final analysis. A period spectrum indicates the best fit period to be 0.645 h, or 38.7 min.

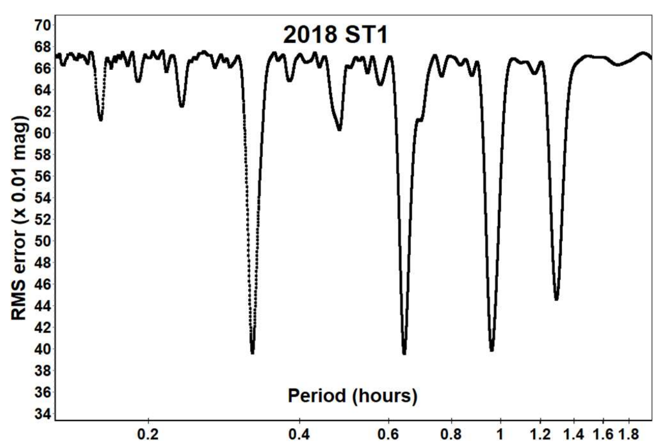

However, the lightcurve, labeled PAR shows significant scatter in places and suggests systematic trends in some of the sets of points.

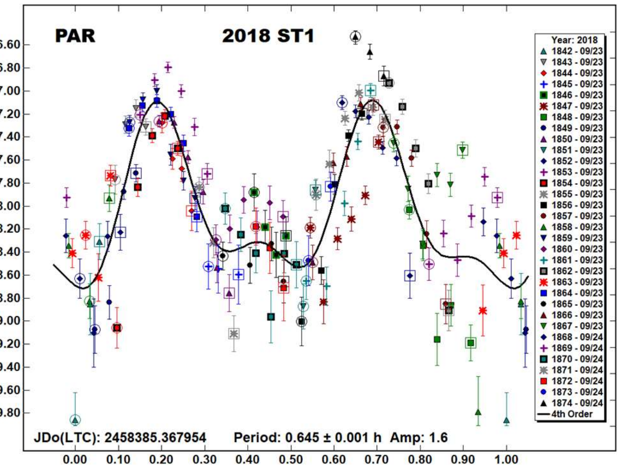

An attempt was therefore made to try and resolve a second period in case non-principal axis (NPA) rotation, or tumbling is present. A number of other less significant minima in the period spectrum hint at solutions and the best fit to a dual-period solution using *MPO Canopus* gives periods of 0.645 and 0.472 h, these two lightcurves are given here, labeled P1 and P2.

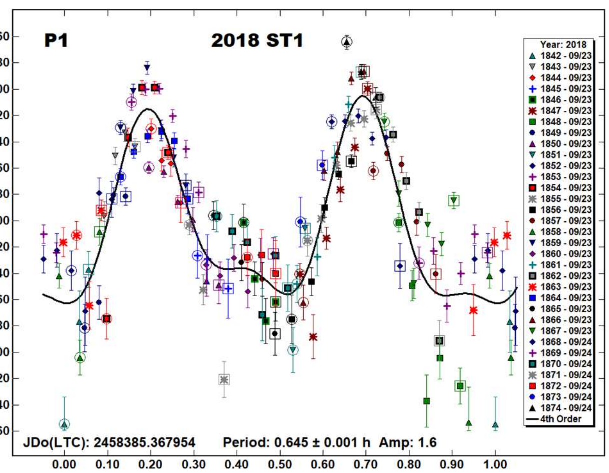

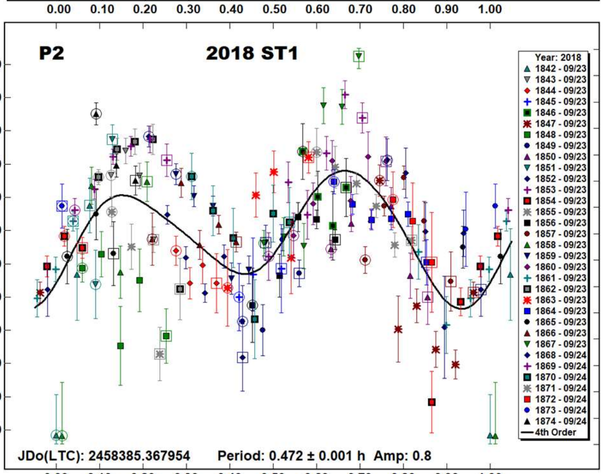

The scatter shown in the dominant and well-defined 0.645 h period P1 lightcurve is reduced but still significant, especially between phase 0.85 and 1.00 and there are obvious problems in the P2 lightcurve throughout. Further attempts at dual-period solutions were less successful and so it is expected that 2018 ST1 may be rated with a PAR code of -2, i.e., *NPA rotation detected based on deviations from the single periodicity but the second period not resolved* (Petr Pravec, personal communication).

The value of H given in the SBDB quotes the MPC derived value of H = 25.1 from MPCORB, based on 43 of the 45 available observations and assuming G = 0.15 (MPC, 2022). The 1-sigma value for the error on H in the SBDB is given as 0.68, presumably a value calculated by JPL, also from the available astrometry, as this is not part of the MPCORB data set. These 43 observations cover a constantly increasing range of phase angles from 38.9 - 98.5°. The lightcurve fitting in this paper results in a value of H_v = 25.6 ± 0.3, also assuming G = 0.15, over phase angles 67.2 - 72.4°. The half magnitude difference in H may be due at least in part to the large observed amplitude, when observed at Great Shefford 2018 ST1 was within 0.1 mag of its predicted peak ephemeris brightness of mag +17.9 and the observed maxima ranged between +17.7 and +16.9 but minima were often +19.5 or fainter. It is possible that the available astrometry may have a bias towards the brighter part of the lightcurve, causing the MPC value of H to be overstated and equivalently, the inferred diameter to be overestimated by ~26%.

<u>2021 LO2</u>. Another small Apollo (H = 28.0, dia. ~7 m) discovered by the Mt. Lemmon Survey on 2021 June 8.33 UTC, it passed Earth at 0.6 LD 5 days later (Bulger et al., 2021). It was observed at a range of 1.4 LD for 70 minutes starting at 2021 June 13.00 UTC. Although relatively bright at 16th magnitude it was at low altitude (17 - 14°), moving rapidly south in a rich star field in southern Ophiuchus and with its apparent speed increasing from 77 to 87 arcsec/min exposures were limited to 5.1 seconds or shorter. Initial analysis with *MPO Canopus* produced the lightcurve labelled PAR, indicating a short rotation period of 41 s. However, multiple minima in the period spectrum suggest there may be tumbling motion present. The period spectrum diagram shows three sets of 4 equally spaced minima, (4 each due to the 4th order Fourier fit utilised) and have been labelled P1, P2 and P3. The 4 minima in each set correspond to monomodal solutions on the left, to quadrimodal on the right and it can be seen that P1, P2 and P3 are commensurate, where approximately (not exactly) 3 P1 = 2 P2 = 1 P3. Using the *MPO Canopus* Dual Period Search function, lightcurves for the dominant P1 period and the next strongest solution, P2 are given here, labelled appropriately. Due to the ambiguity in the secondary solutions, it is expected that 2021 LO2 may be rated with a PAR code of -2, i.e., *NPA rotation detected based on deviations from the single periodicity but the second period not resolved* (Petr Pravec, personal communication).

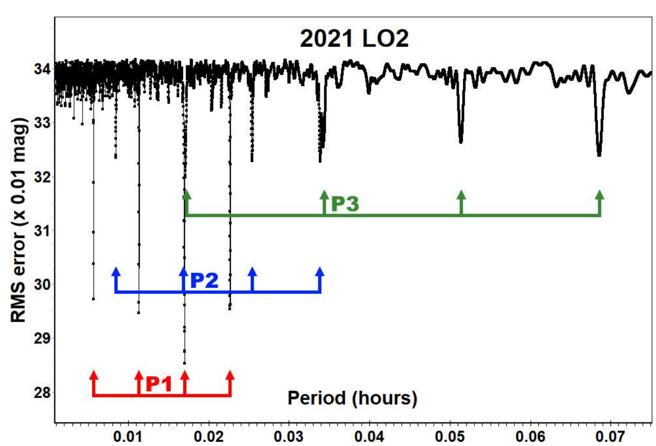

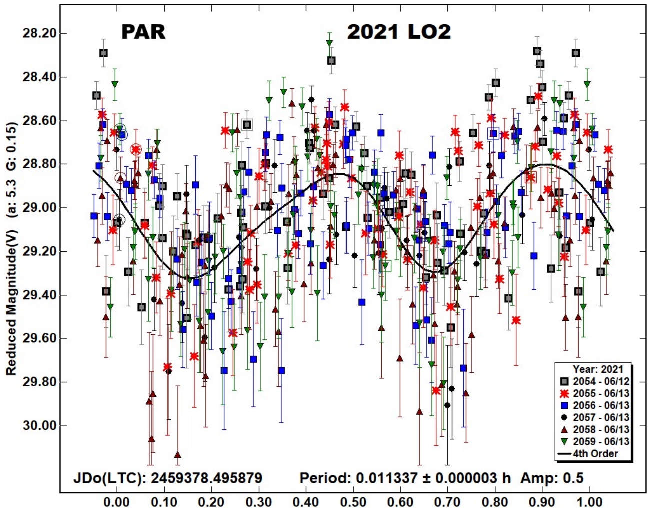

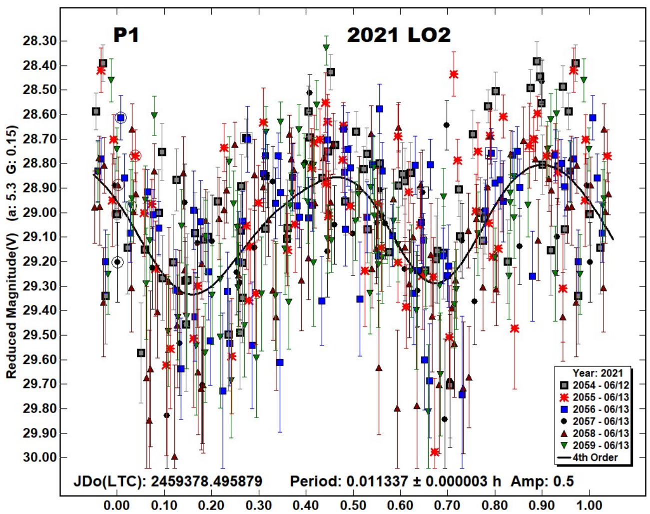

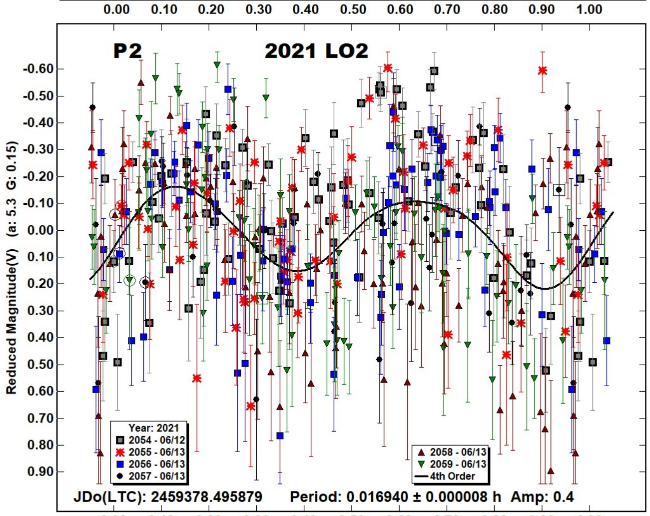

2022 TG. An Apollo with H = 25.1 (estimated dia. ~29 m) which made an approach to within 5 LD of Earth at high southerly declinations 3 days before being discovered by Pan-STARRS 1 on 2022 Oct 2.45 UTC (Coffano et al., 2022). It was observed for 2.8 h starting on 2022 Oct 2.93 UTC when apparent sky motion was 20 arcsec/min. Exposures were 14 s throughout and the telescope was repositioned 6 times. Analysis with *MPO Canopus* indicates a slightly asymmetric bimodal lightcurve and that 14 complete revolutions were covered during the period of observation.

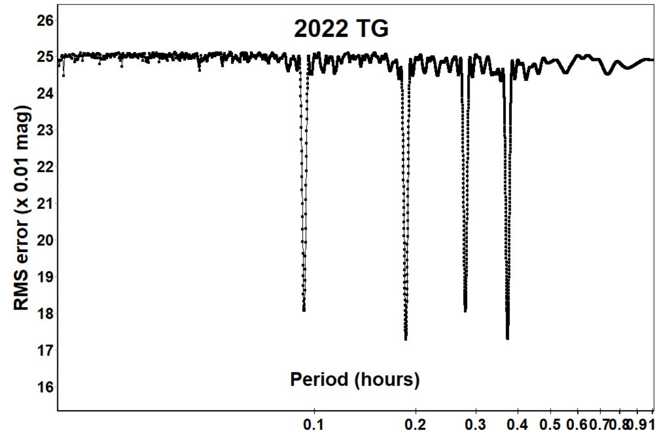

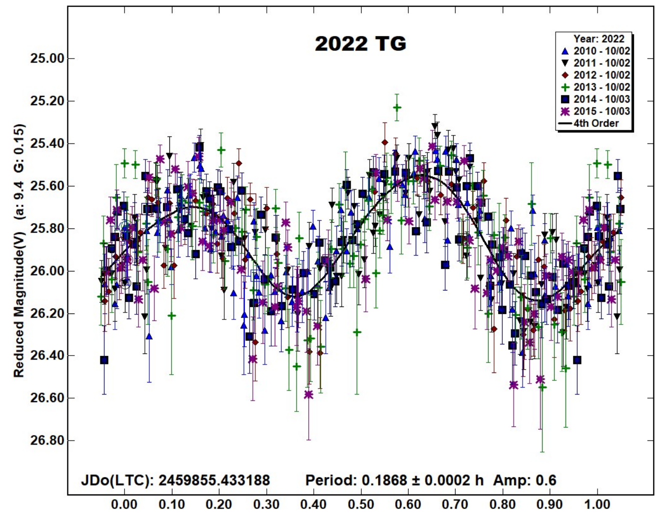

2022 TG1. This was an ATLAS-MLO discovery on 2022 Oct 4.32 UTC made 5 hours after 2022 TG1 passed Earth at 2.8 LD (Bacci et al., 2022). It was observed for a total of 5 h over the nights of 2022 Oct 5 and 6. Initial analysis of the two nights indicated a bimodal lightcurve with a 0.19513 h period, labelled here as PAR. However, both the large amount of scatter in the curve, especially at maxima and also some secondary minima in the period spectrum near 0.13 and 0.26 h suggest there may be tumbling rotation present.

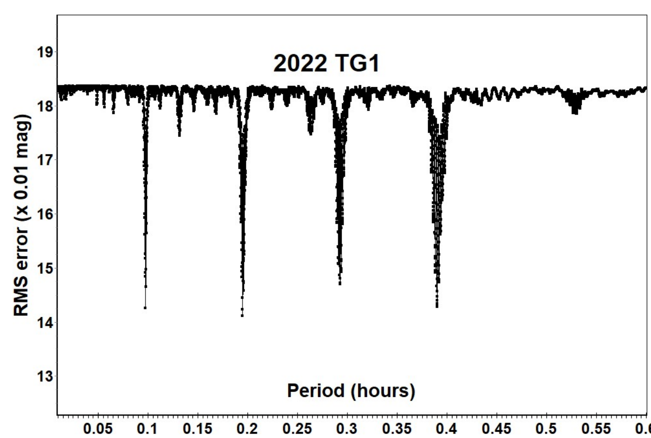

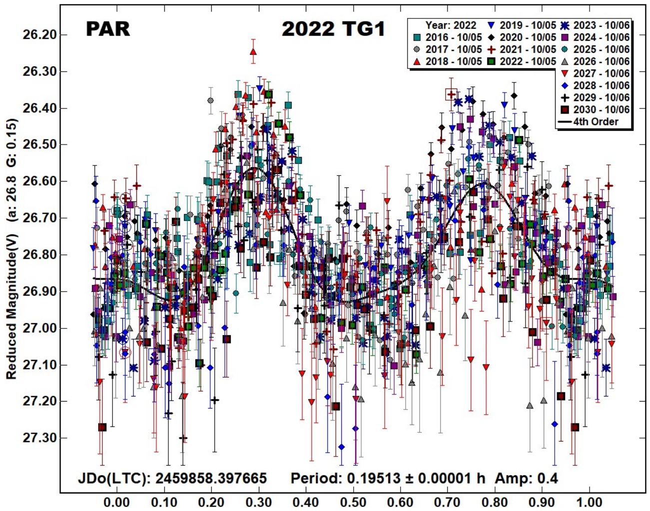

The *MPO Canopus* Dual Period Search was again used and, as well as the dominant 0.19514 h period it also isolated a lower amplitude 0.13176 h secondary period.

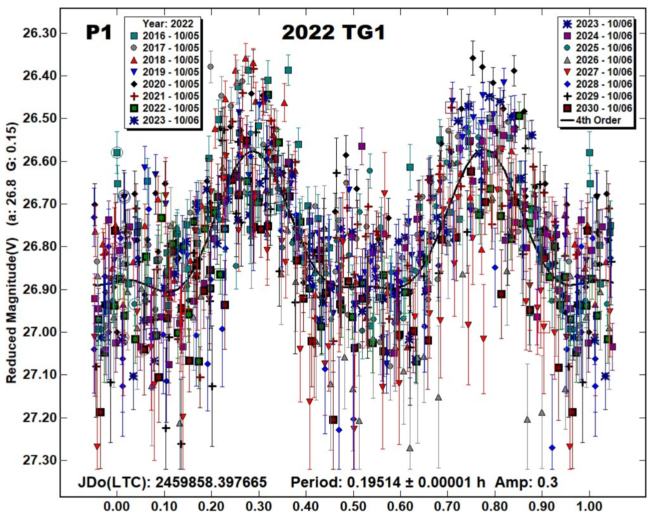

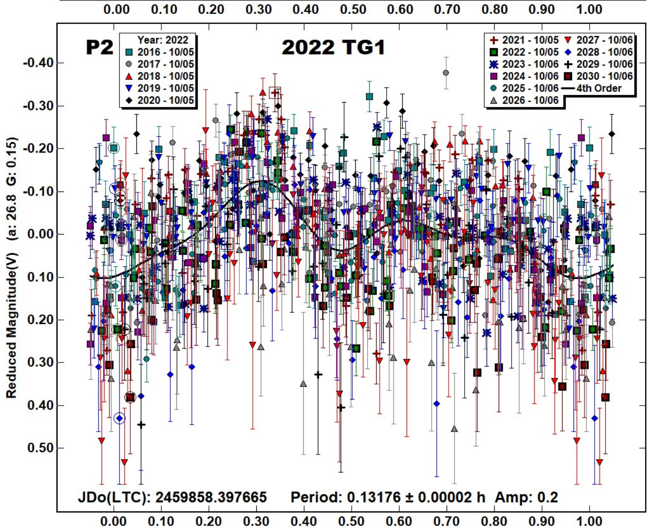

These two curves are given, labelled P1 and P2. It is noted that the two periods are near but not exactly in the ratio 2 P1 = 3 P2. Period P1 is reasonably well defined but the P2 period is not so certain, not helped by the commensurability in the periods, but nevertheless it is clear that 2022 TG1 is tumbling. It is expected that 2022 TG1 may also be rated with a PAR code of -2, i.e., *NPA rotation detected based on deviations from the single periodicity but the second period not resolved* (Petr Pravec, personal communication).

2022 VL1. With H = 26.8 this is a small (~13 m dia.) Apollo, discovered by ATLAS-MLO on 2022 Nov 11.3 UTC (Melnikov et al., 2022) and it passed Earth at 1.2 LD 2 days later on 2022 Nov 13.7 UTC. It was observed for a total of 1.7 h starting on 2022 Nov 12.81 UTC and its apparent speed increased from 75 to 90 arcsec/min. Exposures were reduced from 6.9 to 5.8 seconds to keep the image trails within the measurement annulus in *Astrometrica*. The strongest signals in the period spectrum produced in *MPO Canopus* using a 4th order Fourier fit are multiples of 0.015 h with the best fit being a period of 0.030811 h and the resulting lightcurve is labelled as PAR.

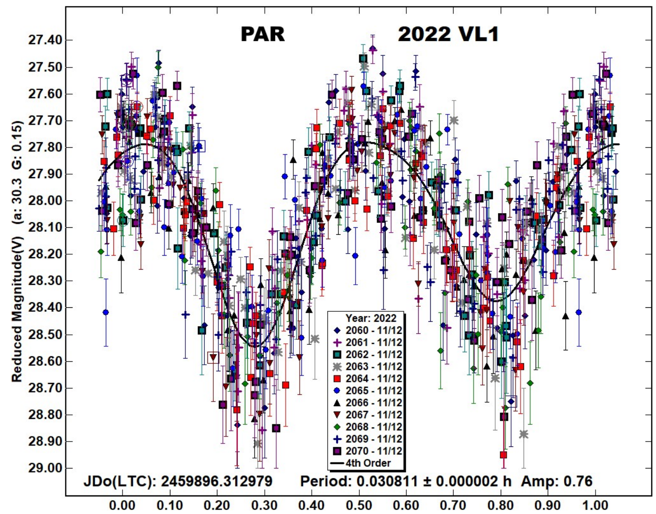

However, the linearly scaled period spectrum also shows a set of weaker solutions at multiples of 0.012 h and using the *MPO Canopus* Dual Period Search two well defined periods of P1 = 0.030811 h and P2 = 0.023860 h are evident and given here labelled P1 and P2.

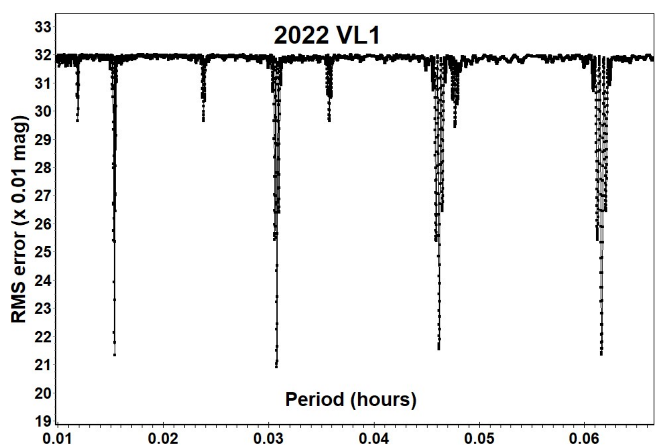

It is therefore expected that it may be rated with a PAR code of -3, i.e., *NPA rotation reliably detected with the two periods resolved*. (Petr Pravec, personal communication).

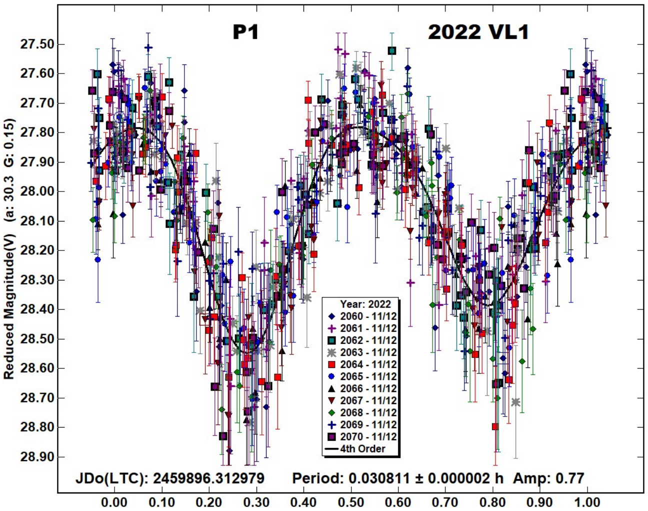

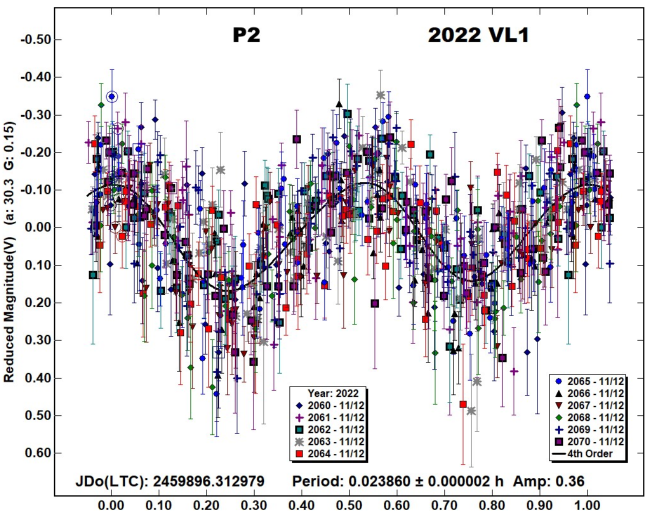

2022 WG5. This Apollo (H = 22.4, est. dia. ~97 m) had been at low solar elongations before being discovered by the Catalina Sky Survey on 2022 Nov 24.51 UTC at a large phase angle of 111°, less than a day after passing Earth at a distance of 4 LD (Serrano et al., 2022). It was observed for 1.0 h starting at 2022 Nov 25.1 UTC when the phase angle had reduced to 96° and for 2.2 h starting 2022 Nov 28.0 UTC at phase angle 65°. Independent period spectrum and phased lightcurve diagrams for the two nights give very similar best fit periods of 0.04413 ± 0.00004 h and 0.04407 ± 0.00001 h, though the shape of the curve has obviously evolved between the two dates. Unusually, the amplitude increased significantly as the phase angle reduced, possibly due to the changing aspect between the two dates if a more equatorial view was presented on the second date compared to the first.

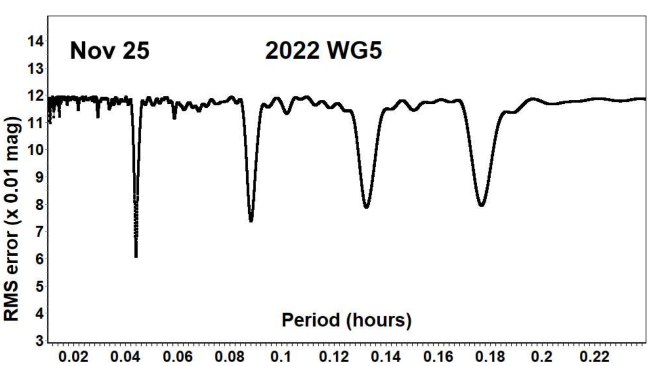

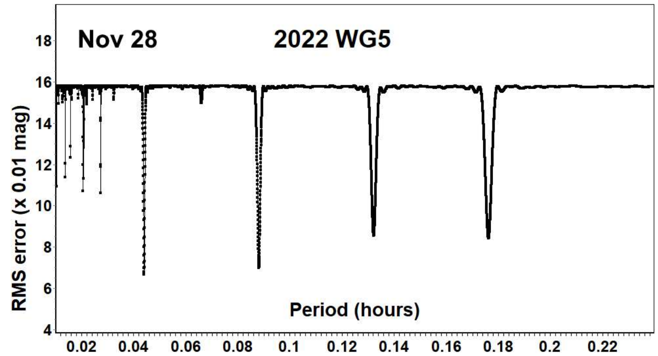

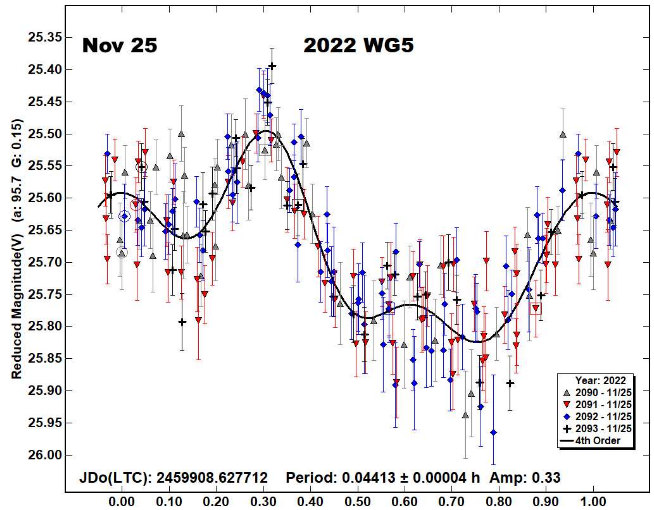

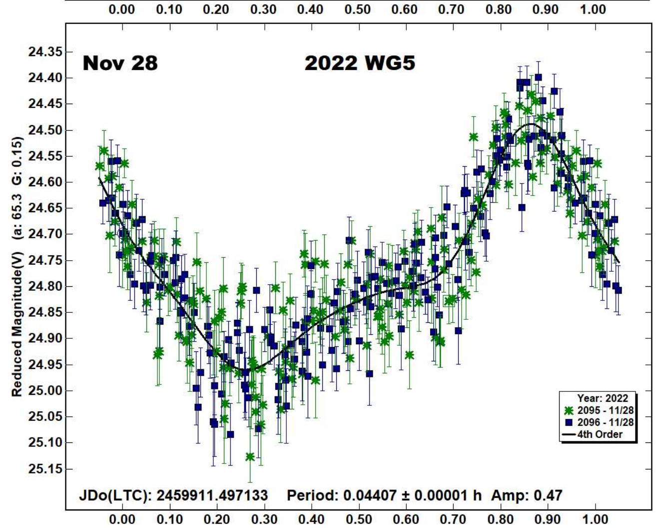

To see whether the results from the two dates could be safely combined to provide a more precise estimate of P, the likely error in number of rotations ΔN between the two dates was again estimated, by propagating the better-defined period from the second date back to the first, using eq. (3) in Kwiatkowski et al. (2010) with the same definitions as given for 2017 TE5:

$$\Delta N \approx \Delta t\ \Delta P / P^2$$

This gives ΔN ≈ 0.34, nominally indicating that, with an error less than half a rotation it should be possible to combine the two data sets unambiguously. However, with the changing shape of the lightcurve and the probable underestimation of the error in P, the actual uncertainty in ΔN is expected to be somewhat larger, therefore, the data from the two dates have not been combined and the value of P from the second date is selected as the most likely result from this analysis.

Acknowledgements

The author wishes to thank Petr Pravec for his generous help and great patience reviewing analyses of tumbling asteroids. The author also gratefully acknowledges a Gene Shoemaker NEO Grant from the Planetary Society (2005) and a Ridley Grant from the British Astronomical Association (2005), both of which facilitated upgrades to observatory equipment used in this study.

Number	Name	Integration times	Max intg/Pd	Min a/b	Pts	Flds
	2003 EM1	4,10	0.090	1.6	97	5
	2008 EZ7	0.6,1	0.017	1.2	189	11
	2011 EY11	0.5,1	0.015	1.4	524	68
	2011 MD	2	0.003	1.3*	585	8
	2012 FP35	0.5,1,2	0.002	1.2	627	28
	2016 GP221	1	0.019	1.3*	124	8
	2017 TE5	2	0.025	1.5	292	4
	2018 SM1	6-16	0.003	1.2*	1017	17
	2018 ST1	260^{Σ}	0.124	1.9*	155	33
	2021 LO2	4.6-5.1	0.125	1.5	396	6
	2022 TG	14	0.021	1.5	468	6
	2022 TG1	14,20	0.028	1.3	594	15
	2022 VL1	5.8-6.9	0.080	1.7	847	11
	2022 WG5	9.2-20	0.126	1.2*	548	7

Table I. Ancillary information, listing the integration times used (seconds), the fraction of the period represented by the longest integration time (Pravec et al., 2000), the calculated minimum elongation of the asteroid (Kwiatkowski et al., 2010), the number of data points used in the analysis and the number of times the telescope was repositioned to different fields. Note: Σ = Longest elapsed integration time for stacked images (start of first to end of last exposure used), * = Value uncertain, based on phase angle > 40°.

References

ADS (2022). Astrophysics Data System. *https://ui.adsabs.harvard.edu/*

Apitzsch, R. (2011web). *http://www.dangl.at/2011/2011_md/2011_md_e.htm*

Bacci, P.; Maestripieri, M.; Grazia, M.D.; Tesi, L.; Fagioli, G.; Ye, Q.-Z.; Briggs, D.; Birtwhistle, P.; Rankin, D.; Wells, G.; Bamberger, D. (2018). "2018 ST1." MPEC 2018-S60. *https://minorplanetcenter.net/mpec/K18/K18S60.html*

Bacci, P.; Maestripieri, M.; Pettarin, E.; Dupouy, P.; de Vanssay, J.B.; Ivanov, A.; Barcov, A.; Ivanov, V.; Lysenko, V.; Yakovenko, N.; Ivanova, N.; Gorbunov, N.; Kurbatov, G.; Shchukin, P.; Ruocco, N. and 24 colleagues (2022). "2022 TG1." MPEC 2022-T73. *https://minorplanetcenter.net/mpec/K22/K22T73.html*

Behrend, R. (2003web). Observatoire de Geneve web site. *http://obswww.unige.ch/~behrend/page5cou.html*

Blythe, M.; Spitz, G.; Brungard, R.; Paige, J.; Festler, P.; McVey, T.; Valdivia, A.; McGaha, J.E.; Sato, H.; Hug, G.; Birtwhistle, P. (2011). "2011 MD." MPEC 2011-M23. *https://minorplanetcenter.net/mpec/K11/K11M23.html*

Bulger, J.; Chambers, K.; Lowe, T.; Schultz, A.; Smith, I.; Chastel, S.; Huber, M.; Ramanjooloo, Y.; Wainscoat, R.; Weryk, R.; Leonard, G.J.; Christensen, E.J.; Farneth, G.A.; Fuls, D.C.; Gibbs, A.R. and 11 colleagues (2021). "2021 LO2." MPEC 2021-L88. *https://minorplanetcenter.net/mpec/K21/K21L88.html*

Buzzi, L.; Tichy, M.; Ticha, J.; Kocer, M.; Honkova, M.; Sakamoto, T.; Hashimoto, N.; Boattini, A.; Ahern, J.D.; Beshore, E.C.; Garradd, G.J.; Gibbs, A.R.; Tricarico, P.; Grauer, A.D.; Hill, R.E. and 8 colleagues (2012). "2012 FP35." MPEC 2012-F78. *https://minorplanetcenter.net/mpec/K12/K12F78.html*

Coffano, A.; Marinello, W.; Micheli, M.; Pizzetti, G.; Soffiantini, A.; Foglia, S.; Galli, G.; Buzzi, L.; Pettarin, E.; Leonard, G.J.; Christensen, E.J.; Fay, D.; Fazekas, J.B.; Fuls, D.C.; Gibbs, A.R. and 54 colleagues (2022). "2022 TG." MPEC 2022-T38. *https://minorplanetcenter.net/mpec/K22/K22T38.html*

Franco, L. (2011web). *https://digilander.libero.it/A81_Observatory/7270/index.html*

Gilmore, A.C.; Kilmartin, P.M.; McGaha, J.E.; Hill, R.E.; Beshore, E.C.; Boattini, A.; Garradd, G.J.; Gibbs, A.R.; Grauer, A.D.; Kowalski, R.A.; Larson, S.M.; McNaught, R.H.; Ries, J.G.; Birtwhistle, P. (2008). "2008 EZ7." MPEC 2008-E67. *https://minorplanetcenter.net/mpec/K08/K08E67.html*

Harris, A.W.; Young, J.W.; Scaltriti, F.; Zappala, V. (1984). "Lightcurves and phase relations of the asteroids 82 Alkmene and 444 Gyptis." *Icarus* **57**, 251-258.

Harris, A.W.; Young, J.W.; Bowell, E.; Martin, L.J.; Millis, R.L.; Poutanen, M.; Scaltriti, F.; Zappala, V.; Schober, H.J.; Debehogne, H.; Zeigler, K. (1989). "Photoelectric Observations of Asteroids 3, 24, 60, 261, and 863." *Icarus* **77**, 171-186.

Hill, R.E.; Ahern, J.D.; Beshore, E.C.; Boattini, A.; Garradd, G.J.; Gibbs, A.R.; Grauer, A.D.; Kowalski, R.A.; Larson, S.M.; McNaught, R.H.; Ryan, W.H.; Ryan, E.V. (2011). "2011 EY11." MPEC 2011-E29. *https://www.minorplanetcenter.net/mpec/K11/K11E29.html*

Janda, M.; Tichy, M.; Bacci, P.; Maestripieri, M.; Grazia, M.D.; Fie, N.; Tesi, L.; Fagioli, G.; Jaeger, M.; Prosperi, E.; Prosperi, S.; Vollmann, W.; Ticha, J.; Matheny, R.G.; Christensen, E.J. and 19 colleagues (2017). "2017 TE5." MPEC 2017-U12. *https://minorplanetcenter.net/mpec/K17/K17U12.html*

JPL (2022a). Small-Body Database Lookup. *https://ssd.jpl.nasa.gov/tools/sbdb_lookup.html*

JPL (2022b). CNEOS NHATS: Accessible NEAs. *https://cneos.jpl.nasa.gov/nhats/details.html#?des=2011%20MD*

Knoefel, A.; Okumura, S.; Nimura, T.; Fuls, D.C.; Christensen, E.J.; Gibbs, A.R.; Grauer, A.D.; Johnson, J.A.; Kowalski, R.A.; Larson, S.M.; Leonard, G.J.; Matheny, R.G.; Seaman, R.L.; Shelly, F.C.; Hug, G. (2016). "2016 GP221." MPEC 2016-G176. *https://minorplanetcenter.net/mpec/K16/K16GH6.html*

Kwiatkowski, T.; Buckley, D.A.H.; O'Donoghue, D.; Crause, L.; Crawford, S.; Hashimoto, Y.; Kniazev, A.; Loaring, N.; Romero Colmenero, E.; Sefako, R.; Still, M.; Vaisanen, P. (2010). "Photometric survey of the very small near-Earth asteroids with the SALT telescope - I. Lightcurves and periods for 14 objects." *Astronomy & Astrophysics* **509**, A94.

Number	Name	yyyy mm/ dd	Phase	L_{PAB}	B_{PAB}	Period(h)	P.E.	Amp	A.E	PAR	H
	2003 EM1	2003 03/06	29.1-28.4	161	14	0.03097	0.00002	1.0	0.2		24.5
	2008 EZ7	2008 03/09	21.5-40.5	183	5	0.016514	0.000002	0.36	0.15		27.0
	2011 EY11	2011 03/06	*15.5-39.2	177	-3	0.0180639	0.0000009	0.7	0.3	-3	28.5
						0.025103	0.000002	0.5	0.3		
	2011 MD	2011 06/27	61.1-60.8	258	26	0.1936	0.0001	0.7	0.1		28.0
	2012 FP35	2012 03/25-03/26	*9.6-22.9	179	3	0.3047	0.0002	0.33	0.15		27.9
	2016 GP221	2016 04/18	65.0-71.6	238	18	0.014973	0.000003	1.0	0.3		25.9
	2017 TE5	2017 10/16-10/17	9.3-16.1	21	5	0.0221191	0.0000006	0.6	0.1		26.0
	2018 SM1	2018 09/26-09/29	64.5-70.7	24	29	1.598	0.001	0.5	0.3	-1	22.9
	2018 ST1	2018 09/23-09/24	67.2-72.4	21	30	0.645	0.001	2.2	0.4	-2	25.1
	2021 LO2	2021 06/12-06/13	5.1-3.9	260	1	0.011337	0.000003	0.5	0.4	-2	28.0
						0.016940	0.000008	0.4	0.4		
	2022 TG	2022 10/02-10/03	9.3-10.0	14	3	0.1868	0.0002	0.6	0.2		25.1
	2022 TG1	2022 10/05-10/06	26.8-26.7	8	13	0.19514	0.00001	0.3	0.2	-2	25.6
						0.13176	0.00002	0.2	0.2		
	2022 VL1	2022 11/12	30.4-30.3	35	-4	0.030811	0.000002	0.8	0.2	-3	26.8
						0.023860	0.000002	0.4	0.2		
	2022 WG5	2022 11/25-11/28	95.9-65.0	96	27	0.04407	0.00001	0.5	0.1		22.4

Table II. Observing circumstances and results. The phase angle is given for the first and last date. If preceded by an asterisk, the phase angle reached an extrema during the period. LPAB and BPAB are the approximate phase angle bisector longitude/latitude at mid-date range (see Harris et al., 1984). Amplitude error (A.E.) is calculated as √2 × (lightcurve RMS residual). PAR is the expected Principal Axis Rotation quality detection code (Pravec et al., 2005) and H is the absolute magnitude at 1 au from Sun and Earth taken from the Small-Body Database Lookup (JPL, 2022a).

Lehmann, G.; Lehmann, K.; Gajdos, S.; Jaeger, M.; Prosperi, E.; Prosperi, S.; Vollmann, W.; Buzzi, L.; Pittichova, J.; Wiggins, P.; Durig, D.T.; Robson, M.; Marmaropoulou, D.; Emmerich, M.; Melchert, S. and 32 colleagues (2018). "2018 SM1." MPEC 2018-S47. *https://minorplanetcenter.net/mpec/K18/K18S47.html*

Melnikov, S.; Hoegner, C.; Ludwig, F.; Stecklum, B.; Tichy, M.; Ticha, J.; Honkova, M.; Janda, M.; Hug, G.; Zoltowski, F.B.; Ikari, Y.; Dupouy, P.; Felber, T.; Birtwhistle, P.; Korlevic, K. and 17 colleagues (2022). "2022 VL1." MPEC 2022-V132. *https://minorplanetcenter.net/mpec/K22/K22VD2.html*

Mommert, M.; Farnocchia, D.; Hora, J.L.; Chesley, S.R.; Trilling, D.E.; Chodas, P.W.; Mueller, M.; Harris, A.W.; Smith, H.A.; Fazio, G.G. (2014). "Physical Properties of Near-Earth Asteroid 2011 MD." *ApJL* **789,** L22.

MPC (2022). Minor Planet Center. MPCORB data file. *https://www.minorplanetcenter.net/iau/MPCORB.html*

Pravec, P.; Hergenrother, C.; Whiteley, R.; Sarounova, L.; Kusnirak, P.; Wolf, M. (2000). "Fast Rotating Asteroids 1999 TY2, 1999 SF10, and 1998 WB2." *Icarus* **147**, 477-486.

Pravec, P.; Harris, A.W.; Scheirich, P.; Kušnirák, P.; Šarounová, L.; Hergenrother, C.W.; Mottola, S.; Hicks, M.D.; Masi, G.; Krugly, Yu.N.; Shevchenko, V.G.; Nolan, M.C.; Howell, E.S.; Kaasalainen, M.; Galád, A. and 5 colleagues. (2005). "Tumbling Asteroids." *Icarus* **173**, 108-131.

Raab, H. (2018). Astrometrica software, version 4.12.0.448. *http://www.astrometrica.at/*

Ryan, E.V.; Ryan, W.H. (2012). Advanced Maui Optical and Space Surveillance Technologies Conference. *http://www.amostech.com/TechnicalPapers/2012/Astronomy/RYAN.pdf*

Serrano, A.; Christensen, E.J.; Fay, D.; Fazekas, J.B.; Fuls, D.C.; Gibbs, A.R.; Grauer, A.D.; Groeller, H.; Hogan, J.K.; Kowalski, R.A.; Larson, S.M.; Leonard, G.J.; Rankin, D.; Seaman, R.L.; Shelly, F.C. and 9 colleagues (2022). "2022 WG5." MPEC 2022-W178. *https://minorplanetcenter.net/mpec/K22/K22WH8.html*

Skiff, B.A.; McLelland, K.P.; Sanborn, J.J.; Koehn, B.W.; Bowell, E. (2022). "Lowell Observatory Near-Earth Asteroid Photometric Survey (NEAPS): Paper 5." *Minor Planet Bulletin* **50**, 74-101.

Tichy, M.; Dintinjana, B.; Skvarc, J.; Gajdos, S.; Toth, J.; Yeung, B.; McClusky, J.; Stevens, B.; Gilmore, A.C.; Kilmartin, P.M.; Sanchez, S.; Stoss, R.; Trentman, R.; Glaze, M.; McGaha, J.E. and 7 colleagues (2003) "2003 EM1" MPEC 2003-E28. *https://minorplanetcenter.net/mpec/K03/K03E28.html*

Vaduvescu, O.; Aznar Macias, A.; Tudor, V.; Predatu, M.; Galád, A.; Gajdoš, Š.; Világi, J.; Stevance, H.F.; Errmann, R.; Unda-Sanzana, E.; Char, F.; Peixinho, N.; Popescu, M.; Sonka, A.; Cornea, R. and 12 colleagues (2017). "The EURONEAR Lightcurve Survey of Near Earth Asteroids." *Earth, Moon, and Planets* **120**, 41-100.

Warner, B.D.; Harris, A.W.; Pravec, P. (2009). "The Asteroid Lightcurve Database." *Icarus* **202**, 134-146. Updated 2021 Dec. *https://minplanobs.org/mpinfo/php/lcdb.php*

Warner, B.D. (2022). MPO Software, Canopus version 10.8.6.12. Bdw Publishing, Colorado Springs, CO.

Zacharias, N.; Finch, C.T.; Girard, T.M.; Henden, A.; Bartlett, J.L.; Monet, D.G.; Zacharias, M.I. (2013). "The Fourth US Naval Observatory CCD Astrograph Catalog (UCAC4)." *The Astronomical Journal* **145**, 44-57.